Proceedings of the 28th IEEE
EMBS Annual International Conference
New York City, USA, Aug 30-Sept 3, 2006

Digital Lock-in Algorithm for Biomedical Spectroscopy and Imaging Instruments with Multiple Modulated Sources

James M. Masciotti, J. M Lasker, A. H. Hielscher

***Abstract*—Digital lock-in detection provides spectroscopic and imaging instruments a means of measuring physical quantities with improved signal to noise ratios compared to analogue detection schemes. We introduce a digital lock-in detection algorithm for measuring the amplitude and phase of multiple amplitude modulated signals simultaneously by using particular modulation and sampling constraints and averaging filters. The technique exhibits exceptional reduction in both noise and inter-source distortion. It is shown that the digital lock-in technique can be performed as a simple matrix multiplication in order to reduce computation time. The digital lock-in algorithm is described and analyzed under certain sampling and modulation conditions. Results are shown for experimental data.**

I. Introduction

Digital lock-in detection [1-6] is utilized in the measurement systems for a wide range of applications. Specific examples are instrumentation for optical spectroscopy [7, 8], diffuse optical tomography [9], electrical impedance spectroscopy [10], and electrical impedance tomography [11]. Instruments for these applications often require the simultaneous measurement of signals from multiple amplitude-modulated sources [12]. Signals often suffer from low signal-to-noise ratios (SNRs) and different modulation frequencies often interfere with each other. In this paper we introduce a digital lock-in detection technique that has features that are ideal for working with multiple modulation frequencies simultaneously. This paper begins with the details of digital lock-in detection for the multiple frequency case. Next, we show that if one uses a mean filter and installs certain constraints on sampling and modulation frequencies, then the digital lock-in detection technique will have certain qualities that are ideal for discriminating between sources at different modulation frequencies. Finally, we will show an alternative way of formulating the digital lock-in technique that will allow for fast computation of amplitude and phase.

This work was supported in part by a grant from the National Institute of Biomedical Imaging and Bioengineering (NIBIB grant 5R01-EB001900) at the National Institutes of Health (NIH) and the Technology Transfer Incentive Program of the New York State Office of Science, Technology and Academic Research.

J. M. Masciotti, J. M. Lasker, and A. H. Hielscher are with Dept. Biomedical Engineering, Columbia University, 500 West 120th Street, New York, NY 10027 USA (phone: 212-854-5738; fax: 212-854-8725; email: jmm2014@columbia.edu)

A. H. Hielscher is also with Dept. Radiology, Columbia University, 660 West 168th Street, New York, NY 10032 USA

II. Digital Lock-in Detection

A. Conventional Digital Lock-in

A system diagram of a multiple modulation frequency digital lock-in detection system is shown in Fig 1. We consider a source signal consisting of multiple modulation frequencies.

$$S(t) = DCs + \sum_{k=1}^{N_m} As_k \cos(2\pi f_k t + \varphi s_k) \tag{1}$$

This source S(t), is input to some target that imposes a change in amplitude and a phase shift on the response which is sampled N_s times at rate f_s to produce the discrete measured signal M[n].

$$M[n] = DCm + \sum_{k=1}^{N_m} A_k \cos\left[\frac{2\pi f_k n}{f_s} + \varphi_k\right] \tag{2}$$

This discrete signal is sent to a computation unit that performs the digital lock-in algorithm. The algorithm can be implemented in hardware on an application-specific integrated circuit (ASIC) or in software. The first step in calculating the amplitude and phase at a given modulation frequency, f_m, is to multiply the discrete signal by some discrete cosine and sine reference signals of the same frequency.

$$C_m[n] = \cos\left[\frac{2\pi f_m n}{f_s}\right] \tag{3}$$

$$S_m[n] = \sin\left[\frac{2\pi f_m n}{f_s}\right] \tag{4}$$

These reference signals can be measured or computed ahead of time and stored in memory. For the technique being presented, they are stored in memory to allow for fast computation and so that they will be free of measurement noise. The results of the multiplication are the so called "nn phase" and "quadrature" or I and Q signals.

$$I_m[n] = \sum_{k=1}^{N_m} DC_m \cos\left[\frac{2\pi f_m}{f_s}\right] + \frac{A_k}{2}\left(\cos\left[\frac{2\pi(f_m - f_k)n}{f_s} + \varphi_k\right] + \cos\left[\frac{2\pi(f_m + f_k)n}{f_s} + \varphi_k\right]\right) \tag{5}$$

$$Q_m[n] = \sum_{k=1}^{N_m} DC_m \sin\left[\frac{2\pi f_m}{f_s}\right] + \frac{A_k}{2}\left(\sin\left[\frac{2\pi(f_m - f_k)n}{f_s} + \varphi_k\right] + \sin\left[\frac{2\pi(f_m + f_k)n}{f_s} + \varphi_k\right]\right) \tag{6}$$

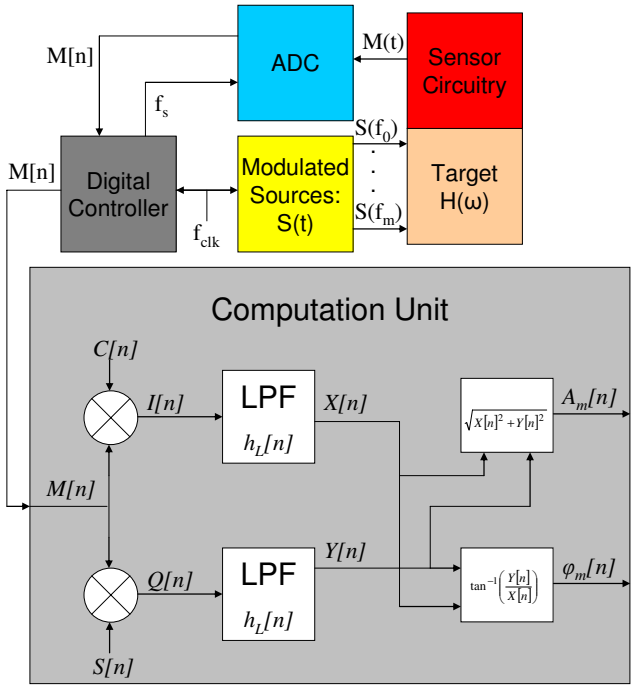

Figure 1: Diagram of digital lock-in detection hardware and algorithm to be implemented in the digital domain. A source S(t) is modulated at frequencies f_0 to f_m and is input to a target. A signal is measured M(t) by the sensor and then it is sampled into a discrete signal M[n] by the ADC. The computation unit performs the digital lock-in algorithm and calculates the amplitude A_m and phase φ_m.

The amplitude and phase can be calculated from the DC terms in $I_m[n]$ and $Q_m[n]$, which are passed through a lowpass filter in order to remove the higher order terms and yield $X_m[n]$ and $Y_m[n]$.

$$X_m[n] = h_L[n] \otimes I_m[n] \tag{7}$$

$$Y_m[n] = h_L[n] \otimes Q_m[n] \tag{8}$$

$X_m[n]$ and $Y_m[n]$ will each consist of a DC term and higher frequency terms that will be attenuated by the lowpass filter. The objective of the lowpass filter is to eliminate these high-frequency terms altogether and yield just the DC terms:

$$X_m[n] \approx \frac{1}{2} A_m \cos(\varphi_m) \tag{9}$$

$$Y_m[n] \approx \frac{1}{2} A_m \sin(\varphi_m) \tag{10}$$

The amplitude Am and phase can be calculated by:

$$A_m[n] = 2 * \sqrt{X[n]^2 + Y[n]^2} \tag{11}$$

$$\varphi_m[n] = -\tan^{-1}\left(\frac{Y[n]}{X[n]}\right) \tag{12}$$

B. *Averaging filter*

It is well known that for white noise, the optimum lowpass FIR filter is the simple averaging filter which has equal coefficients at each of its Ns points [13].

$$h_L[n] = \frac{1}{N_s} \tag{13}$$

The frequency response of the averaging filter is given by:

$$H(f) = \frac{\sin\left(\frac{N_s \pi f}{f_s}\right)}{\sin\left(\frac{\pi f}{f_s}\right)} e^{-j\frac{\pi(N_s-1)f}{f_s}} \tag{14}$$

As with any digital lowpass filter, the stop-band attenuation will be proportional to its time constant, N_s/f_s, and the higher the sampling frequency the less high frequency noise aliases over into the pass-band. For N_s larger than 10, the bandwidth is approximately $.443 f_s/N_s$. For the averaging filter, random white noise on a discrete signal will be attenuated by the square root of the number of samples N_s.

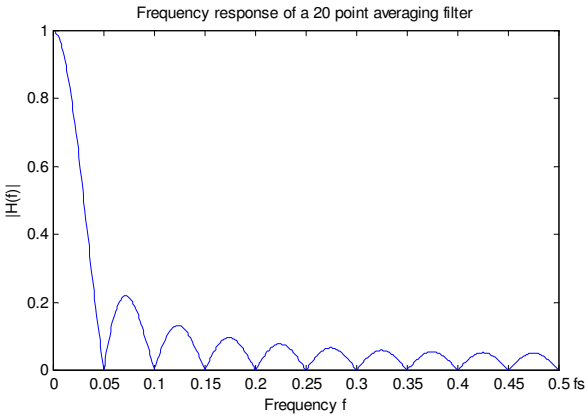

Figure 2: Frequency response of a 20 point averaging filter which has zeros at multiples of f_s/N_s.

The dc value computed by an averaging filter will not equal the true dc value. As is evident by the frequency response of the 20 point averaging filter shown in Fig. 2, some AC frequency components will not be filtered out entirely and will distort the result. This is a serious issue because the $I_m[n]$ and $Q_m[n]$ signals will contain many frequency components that will distort $X_m[n]$ and $Y_m[n]$. One does observe, however, that the N_s point averaging filter has a response of zeros at integer multiples of f_s/N_s which correspond to frequencies that are sampled for integer number of periods. This advantageous property can be exploited with particular sampling constraints.

C. *Modulation and Sampling Constraints*

$X_m[n]$ and $Y_m[n]$ can be freed from distortion from the other modulation frequencies by making sure that all of the AC terms in $I_m[n]$ and $Q_m[n]$ occur at frequencies at which the response of the averaging filter is zero. This can be accomplished by constraining all of the modulation frequencies, f_m, by:

$$f_m = \frac{k f_s}{N_s} \quad 1 \le k < \frac{N_s}{2} \tag{15}$$

where k is some integer. In this way, all of the AC terms in $I_m[n]$ and $Q_m[n]$ will also be multiples of f_s/N_s and will be

filtered out completely by the averaging filter. This is evident in Fig. 3 where signals from two modulation frequencies are shown along with how there corresponding $I_m[n]$ signals overlap with the frequency response of the averaging filter. Notice that after modulation all of the AC terms are shifter to frequencies where the frequency response is zero. For these unwanted frequencies to be filtered out completely, it is important that there is no error in modulation frequency relative to the sampling frequency. This can be assured, by running both the digital controller that triggers the ADC to sample and the circuitry that modulates the source, off of the same clock. A constraint now arises between the modulation frequency and the number of clock cycles between sampling triggers:

$$f_m = \frac{kf_{clk}}{N_s N_c}, 1 \le k < \frac{N_s}{2} \tag{16}$$

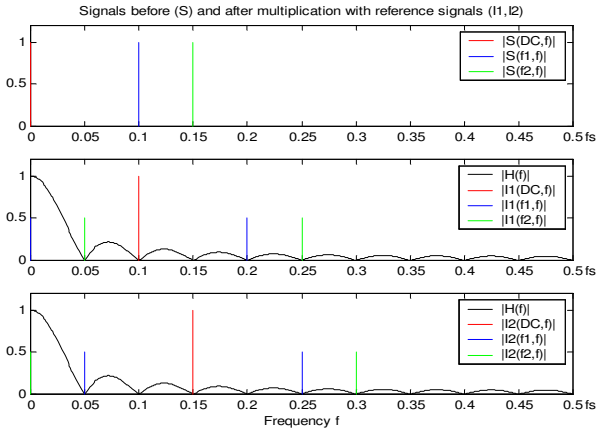

Figure 3: Frequency domain representation of DC (red), first frequency (f1) (blue) and second frequency (f2) (green) components before and after they have been multiplied by the reference to produce $I_m[n]$ signals. Fig. 3a: Components of the original signal. Fig. 3b: Components of the $I_1[n]$ signal due to multiplication with the first reference signal overlaid on the averaging filter frequency response. Fig. 3c: Components of the $I_2[n]$ signal due to multiplication with the second reference signal overlaid on the averaging filter frequency response.

D. Computation Issues

Computation time for real-time digital lock-in detection of numerous channels at multiple modulation frequencies can become an issue. At first, it might appear computationally intensive. However, the whole process of multiplying an N_s point measurement with the N_s point reference signals and taking the average can be performed by the following simple matrix multiplications which can of implemented very efficiently.

$$\begin{bmatrix} X_1 \\ X_2 \\ \vdots \\ X_{N_m} \end{bmatrix} = \frac{1}{N_s} \begin{bmatrix} 1 & \cos\left(\frac{2\pi f_1}{f_s}\right) & \cdots & \cos\left(\frac{2\pi f_1 (N_s-1)}{f_s}\right) \\ 1 & \cos\left(\frac{2\pi f_2}{f_s}\right) & \cdots & \cos\left(\frac{2\pi f_2 (N_s-1)}{f_s}\right) \\ \vdots & \vdots & \ddots & \vdots \\ 1 & \cos\left(\frac{2\pi f_{N_m}}{f_s}\right) & \cdots & \cos\left(\frac{2\pi f_{N_m} (N_s-1)}{f_s}\right) \end{bmatrix} \times \begin{bmatrix} M[1] \\ M[2] \\ \vdots \\ M[N_s] \end{bmatrix} \tag{17}$$

$$\begin{bmatrix} Y_1 \\ Y_2 \\ \vdots \\ Y_{N_m} \end{bmatrix} = \frac{1}{N_s} \begin{bmatrix} 0 & \sin\left(\frac{2\pi f_1}{f_s}\right) & \cdots & \sin\left(\frac{2\pi f_1 (N_s-1)}{f_s}\right) \\ 0 & \sin\left(\frac{2\pi f_2}{f_s}\right) & \cdots & \sin\left(\frac{2\pi f_2 (N_s-1)}{f_s}\right) \\ \vdots & \vdots & \ddots & \vdots \\ 0 & \sin\left(\frac{2\pi f_{N_m}}{f_s}\right) & \cdots & \sin\left(\frac{2\pi f_{N_m} (N_s-1)}{f_s}\right) \end{bmatrix} \times \begin{bmatrix} M[1] \\ M[2] \\ \vdots \\ M[N_s] \end{bmatrix} \tag{18}$$

Interestingly enough, the rows of the matrices correspond to rows of the real and imaginary parts of the DFT matrix that are needed to compute the DFT at that particular modulation frequency. For computational units that allow efficient computation of complex numbers, the rows of the DFT matrix can be used directly.

$$\begin{bmatrix} X_1 - jY_1 \\ X_2 - jY_2 \\ \vdots \\ X_3 - jY_{N_m} \end{bmatrix} = \frac{1}{N_s} \begin{bmatrix} 1 & e^{\left(\frac{-j2\pi f_1}{f_s}\right)} & \cdots & e^{\left(\frac{-j2\pi f_1 (N_s-1)}{f_s}\right)} \\ 1 & e^{\left(\frac{-j2\pi f_2}{f_s}\right)} & \cdots & e^{\left(\frac{-j2\pi f_2 (N_s-1)}{f_s}\right)} \\ \vdots & \vdots & \ddots & \\ 1 & e^{\left(\frac{-j2\pi f_{N_m}}{f_s}\right)} & \cdots & e^{\left(\frac{-j2\pi f_{N_m} (N_s-1)}{f_s}\right)} \end{bmatrix} \times \begin{bmatrix} M[1] \\ M[2] \\ \vdots \\ M[N_s] \end{bmatrix} \tag{17}$$

The amplitude and phase are then calculated as magnitude and angle of a complex number, resulting in the same equations as in (11) and (12).

III. Results

To test the algorithm, 2 light emitting diodes (LEDs) were amplitude modulated at frequencies of 5 kHz and 7 kHz to produce an amplitude of approximately 1. The signal was measured by a photodetector with a transimpedance amplifier and the signal was sampled by an oscilloscope and saved into memory. The sampling frequency f_s was set to 50 kHz and N_s = 100 samples were taken. The digital lock-in algorithm was implemented in MATLAB on a PC with an AMD Athlon™ XP processor. Fig. 4 shows measured signals (black) and signals that are reconstructed from calculated amplitude and phase (blue). The lock-in algorithm was run on single and multiple modulation frequency data. Fig. 4a shows a 5 kHz signal with an SNR of 11 and a calculated amplitude of 1.0016. Fig. 4b shows a 7 kHz signal with an SNR or 7.9 and a calculated amplitude of 1.. Fig. 4c shows the effectiveness of the algorithm with multiple frequencies at once. The signals from Fig. 4a and Fig. 4b were added together with a resulting SNR is 6.5. The calculated amplitude 5 kHz signal is 1.00526 while the calculated amplitude and phase for the 7 kHz signal is 0.9975. These showed a variation with the single modulation data of only 0.37% and 0.3% which well below the noise level. Also, the algorithm was tested in both the conventional multiply-and-take-the-mean form and the matrix multiplication form in (17) and (18). The matrix

multiplication-method performed 200 times faster than the conventional method even though both yielded the exact same amplitude and phase results.

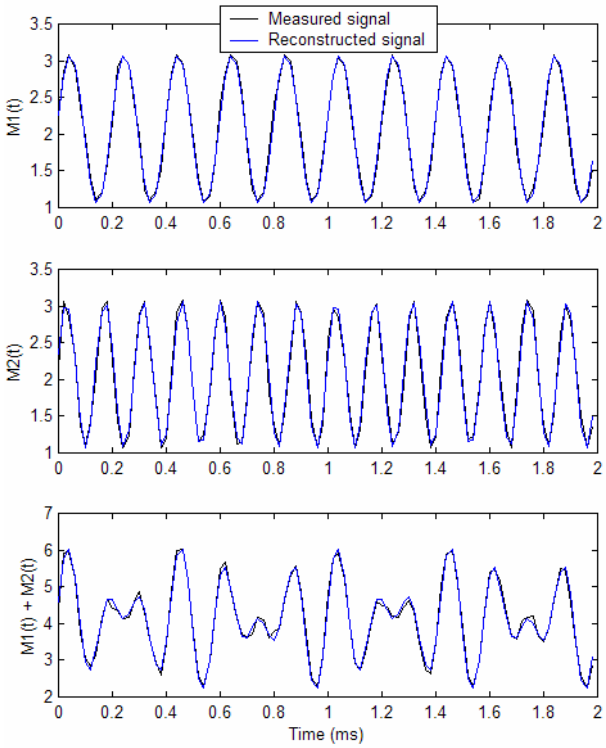

Figure 4: Shows measured signals (black) and signals that are synthesized from calculated amplitude and phase (blue). Fig. 4a shows the measured 5 kHz signal with the signal reconstructed from its amplitude and phase. Fig. 4b shows the measured 7 kHz signal with the signal reconstructed from its amplitude and phase. Fig. 4c shows the measured signal consisting of both a 5 kHz and 7 kHz signal along with the signal reconstructed from there respective calculated amplitudes and phase.

IV. Conclusion

We presented a digital lock-in amplification detection scheme that is optimal for many applications, particularly biomedical spectroscopy and imaging. The digital lock-in detection scheme utilizes sampling and modulation constraints and the unique frequency response of the averaging filter to provide excellent white-noise cancellation and source discrimination. It was shown that the digital lock-in technique can measure the amplitude and phase at multiple frequencies without them distorting each other. It was also shown that implementing the technique as a matrix multiplication yields a substantial increase in speed.

References

[1] E. D. Morris, H. S. Johnston, "Digital Phase Sensitive Detector", Rev. Sci. Instrum.. 39, 620 -621 (1968).

[2] G. D.Renkes, L. R. Thorne, W. D. Gwinn, "Digital Modulator and synchronous demodulator system: an alternative to the analog phase detector", Rev. Sci. Instrum., 49, 994-1000 (1976).

[3] S. Carrato, G. Paolucci, R. Tommsini, R. Rosei, "Versatile low-cost digital lock-in amplifier suitable for multichannel phase sensitive detection", Rev. Sci. Instrum., 60, 2257-2259 (1989).

[4] F. Barone, E. Calloni, L. DiFiore, A. Grado, L. Milano, G. Russo, "High-performance modular digital lock-in amplifier", Rev. Sci. Instrum., 66, 3697 – 3702 (1995).

[5] L. A. Barragan, J. I. Artigas, R. Alonso, F. Villuendas, "A modular, low-cost, digital signal processor-based lock-in card for measuring optical attenuation" Rev. Sci. Instrum., 72, 247 – 251 (2001).

[6] L. A. Barragan, J. I. Artigas, R. Alonso, F. Villuendas, "A modular, low-cost, digital signal processor-based lock-in card for measuring optical attenuation" Rev. Sci. Instrum., 72, 247 – 251 (2001).

[7] S. Cova, A. Longoni, I. Freitas, "Versatile digital lock-in detection technique: Application to Spectorflourometry and other fields", Rev. Sci. Instrum., 50, 296 – 301 (1979).

[8] R. Alonso, F. Villuendas, J. Borja, L. A. Barragan, I Salinas, "Low-cost, digital lock-in module with external reference for coating glass transmission/reflection spectrophotometer" Meas. Sci. Technol. 14, 551 – 557 (2003).

[9] B. W. Pogue, M. Testorf, T. McBride, U. Osterberg, K. Paulsen, "Instrumentation and design of a frequency domain diffuse optical tomography imager for breast cancer detection", Opt. Express, 1, 391 – 403 (1997).

[10] A. Albertini, W. Kleeman, "Analogue and digital techniques for very-low-frequency impedance spectroscopy", Meas. Sci. Technol. 8, 666 – 672, (1997).

[11] T. I Oh, J. W. Lee, K. S. Kim, J. S. Lee, E. J. Wu, "Digital Phase-Sensitive Modulator for Electrical Impedance Tomography", *Proceedings of the 25th Annual International Conference of the IEEE EMBS*, IEEE, Cancun, Mexico, September 17 – 21, 2003.

[12] C. H. Schmitz, M. Locker, J. M. Lasker, A. H. Hielscher, R. L. Barbour, "Instrumentation for fast functional optical Tomography", Rev. Sci. Instrum. 73, 429 – 439 (2002).

[13] O. Vaino, "Minimum-Phase FIR Filters for Delayed Constrained Noise Reduction", IEEE Trans. Instrum. Meas., 48, 1100-1102 (1999).